Cell & Tissue Research Springer

Ultrastructural and immunocytochemical evidence for the reorganisation of the Milk Fat Globule Membrane after secretion.

Journal:	*Cell and Tissue Research*
Manuscript ID	CTR-16-0124.R1
Manuscript Type:	Regular Article
Date Submitted by the Author:	24-May-2016
Complete List of Authors:	Wooding, F. B. Peter; cambridge university, physiology MATHER, Ian ; University of Maryland at College Park, Department of Animal and Avian Sciences
Keywords:	milk fat globule membrane, ultrastructure, immunocytochemistry, paracrystalline arrays, unit membrane

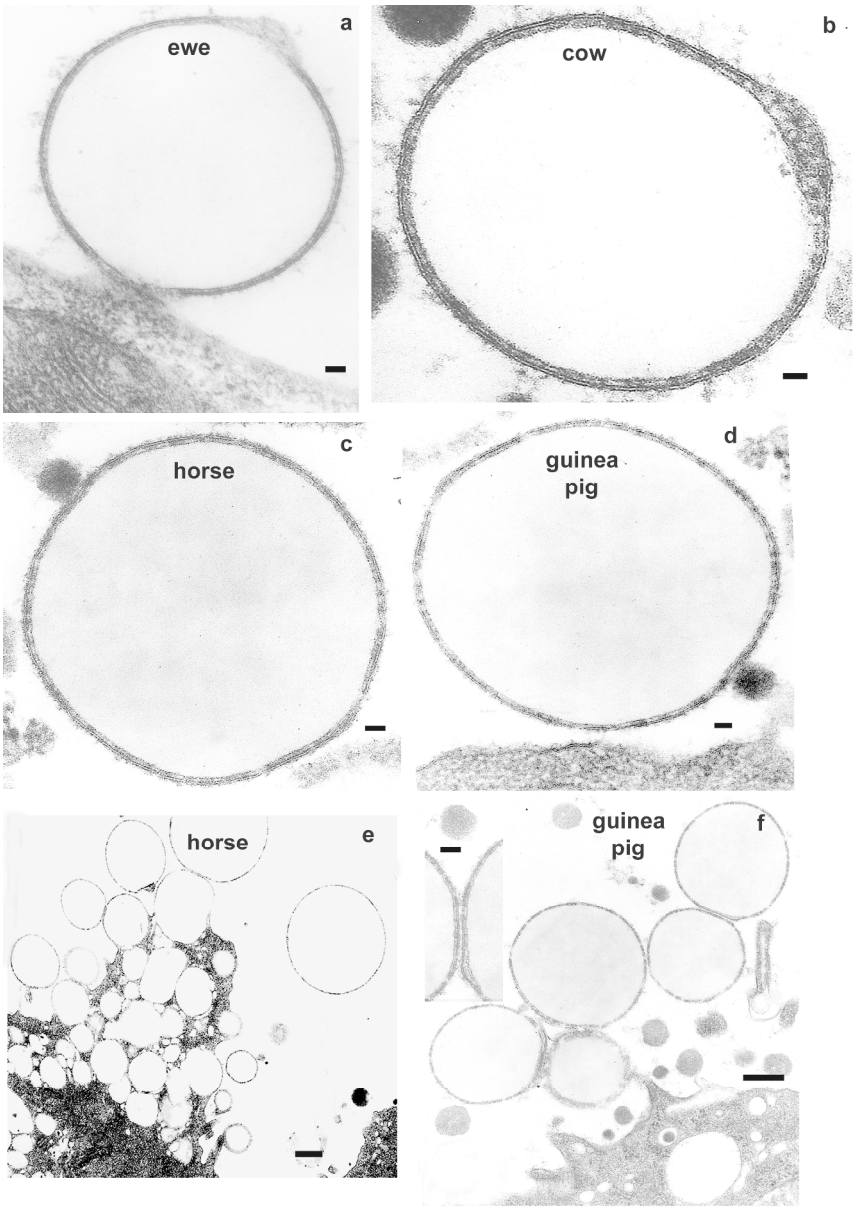

Fig. 1
209x297mm (300 x 300 DPI)

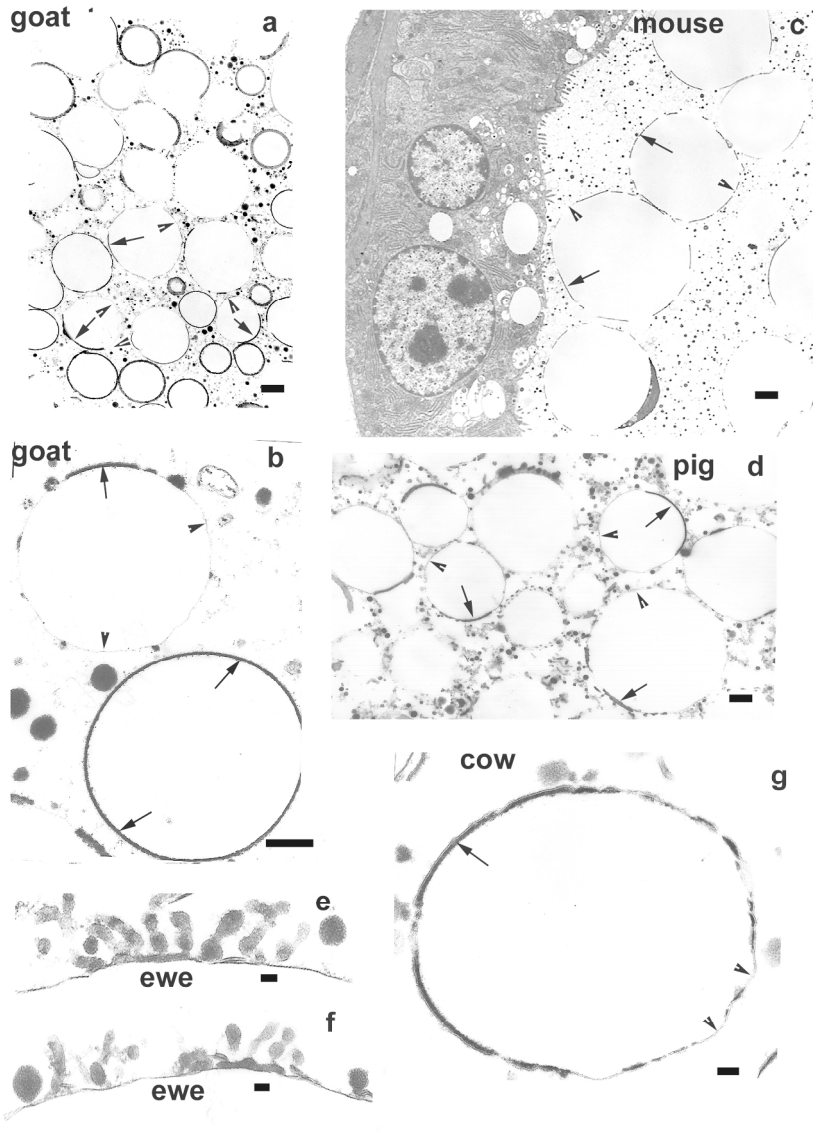

Fig. 2
163x236mm (300 x 300 DPI)

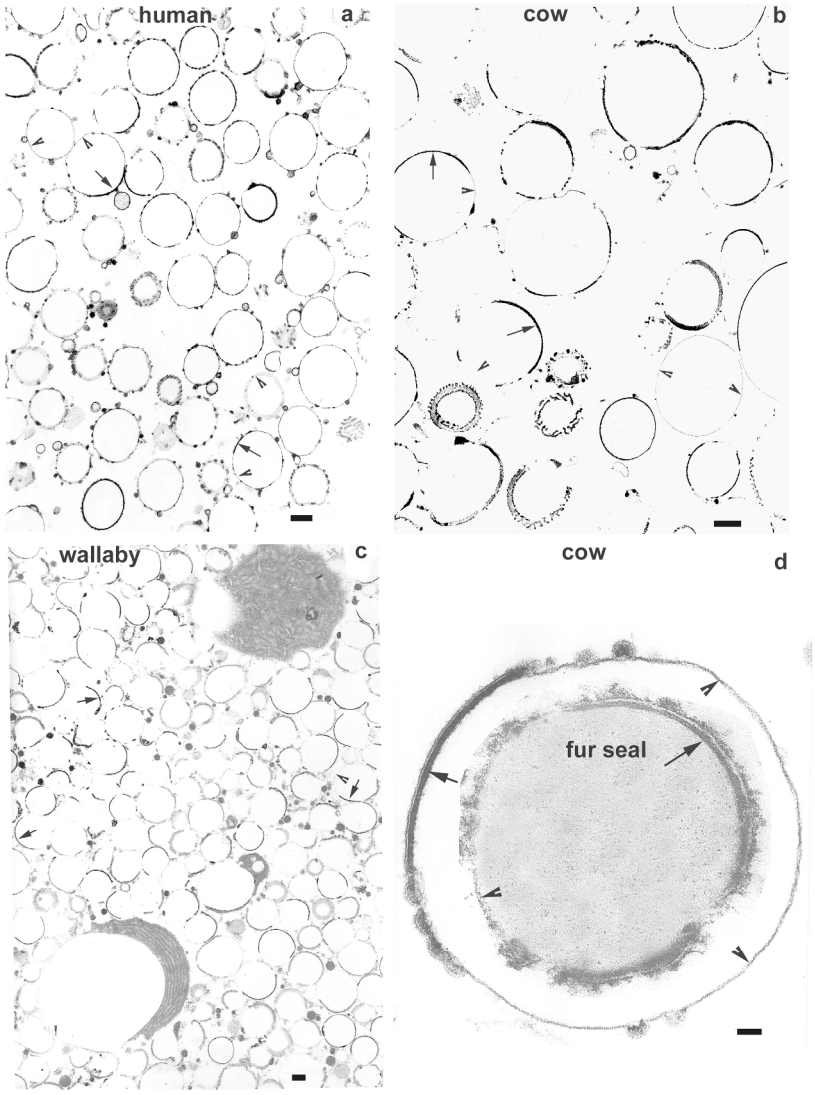

Fig. 3
209x297mm (300 x 300 DPI)

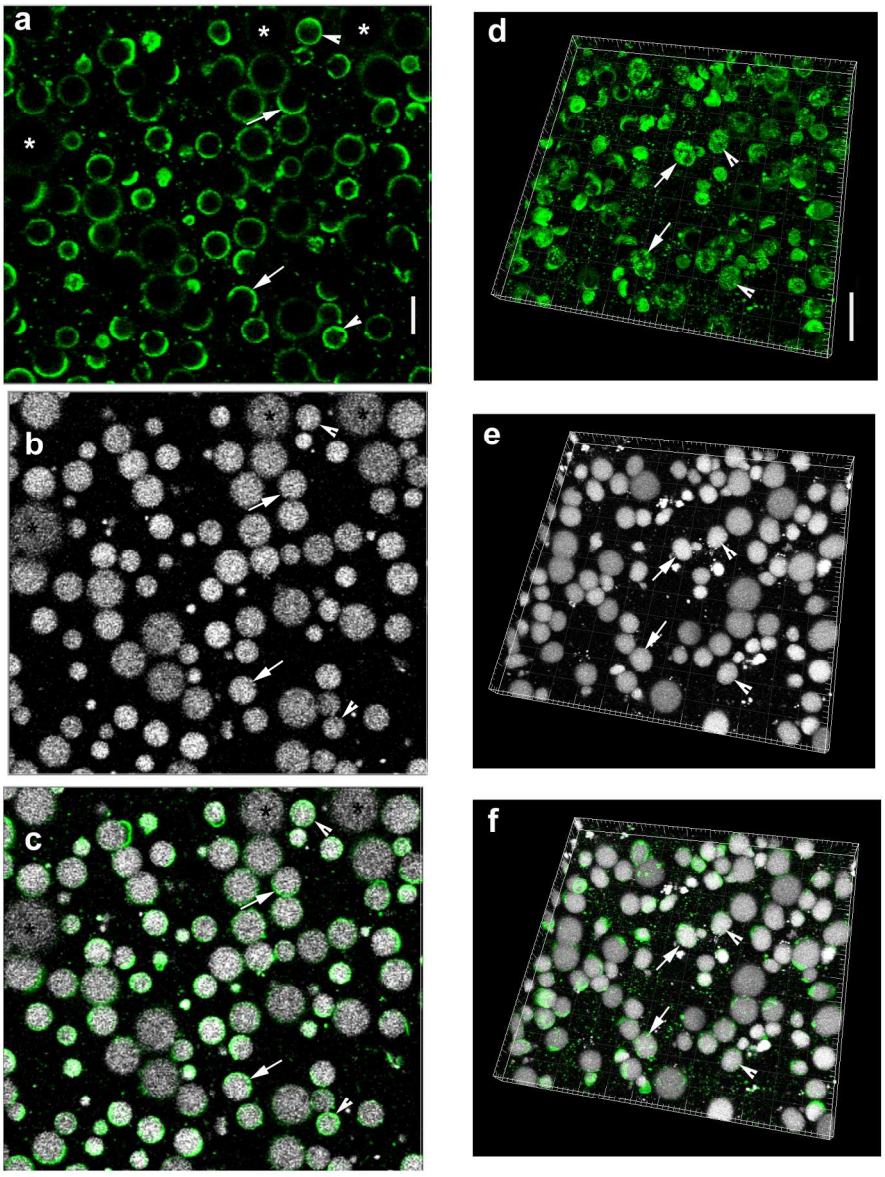

Fig. 4
162x207mm (300 x 300 DPI)

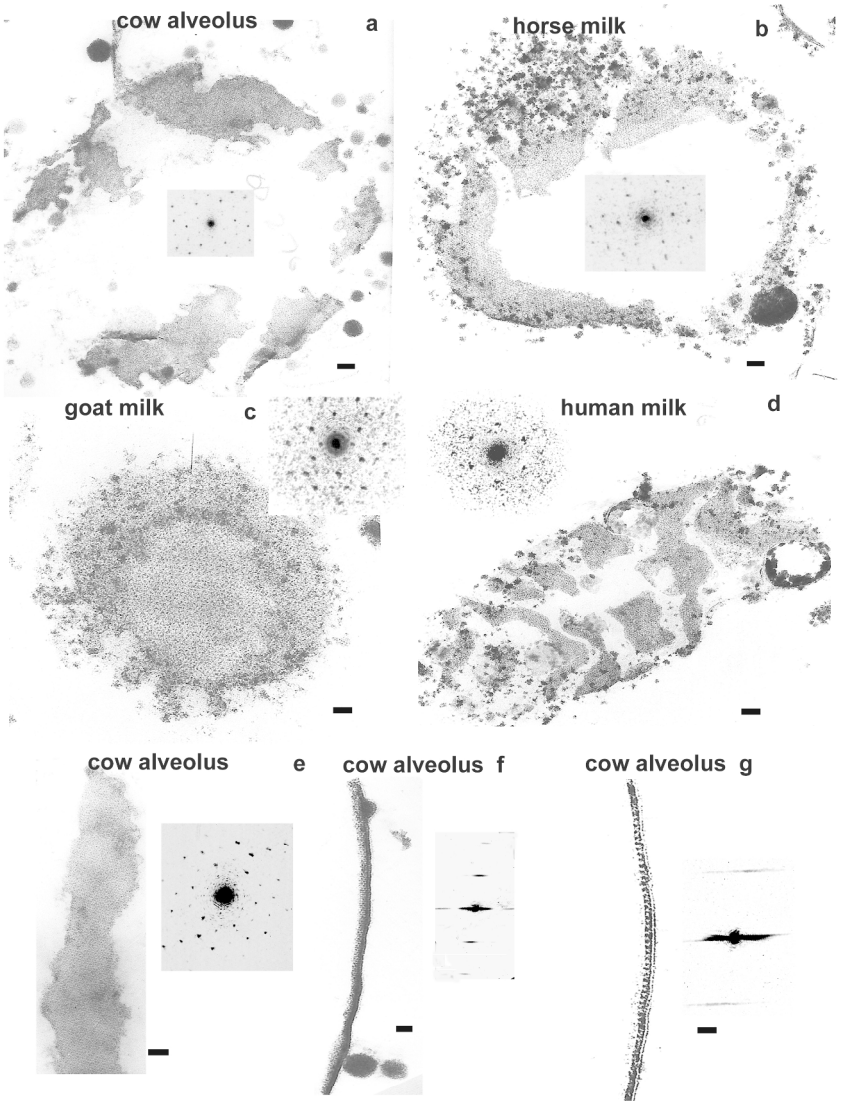

Fig. 5
209x297mm (300 x 300 DPI)

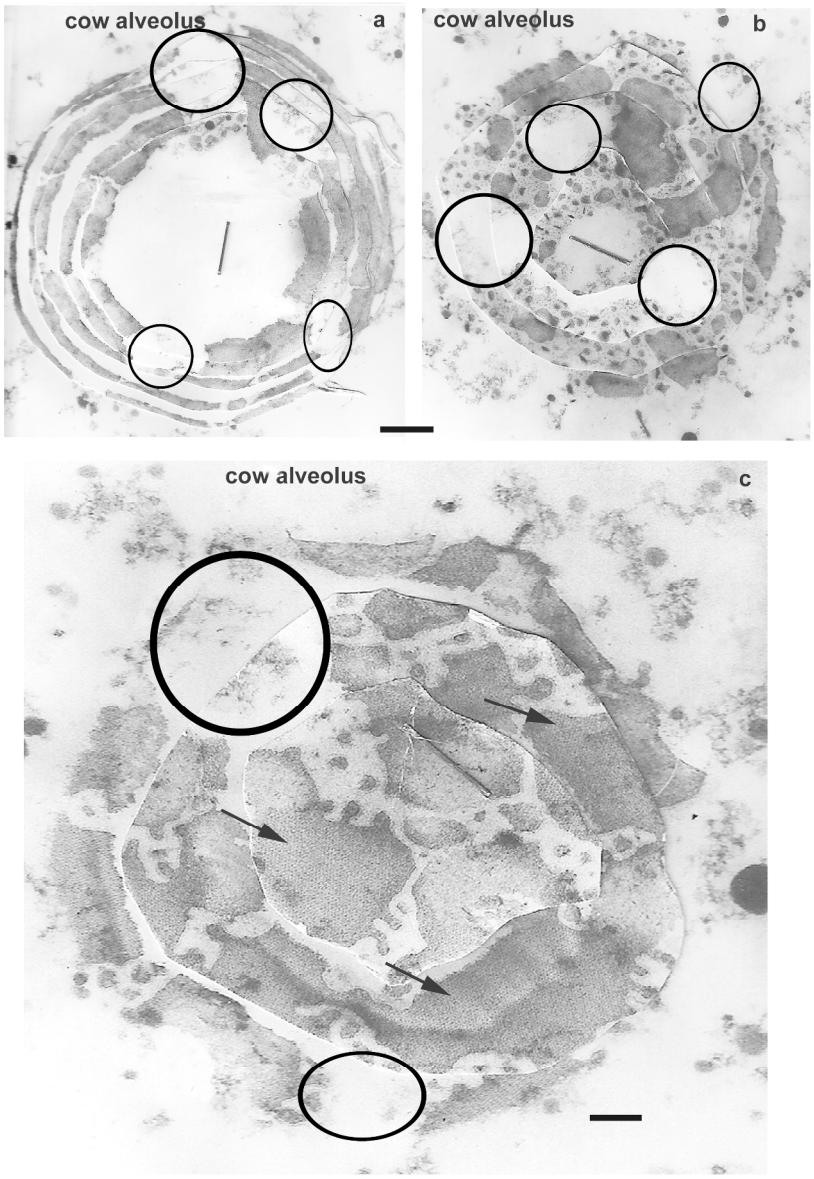

Fig. 6
209x297mm (300 x 300 DPI)

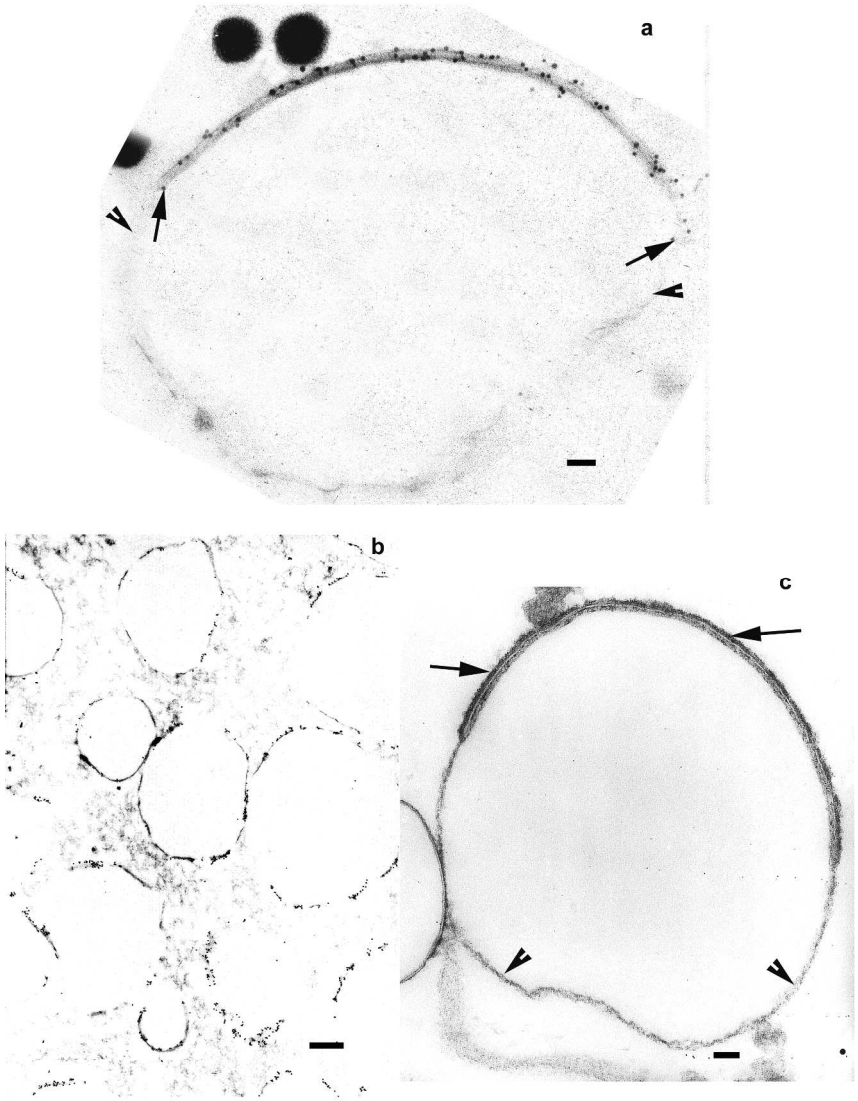

Fig. 7
874x1237mm (72 x 72 DPI)

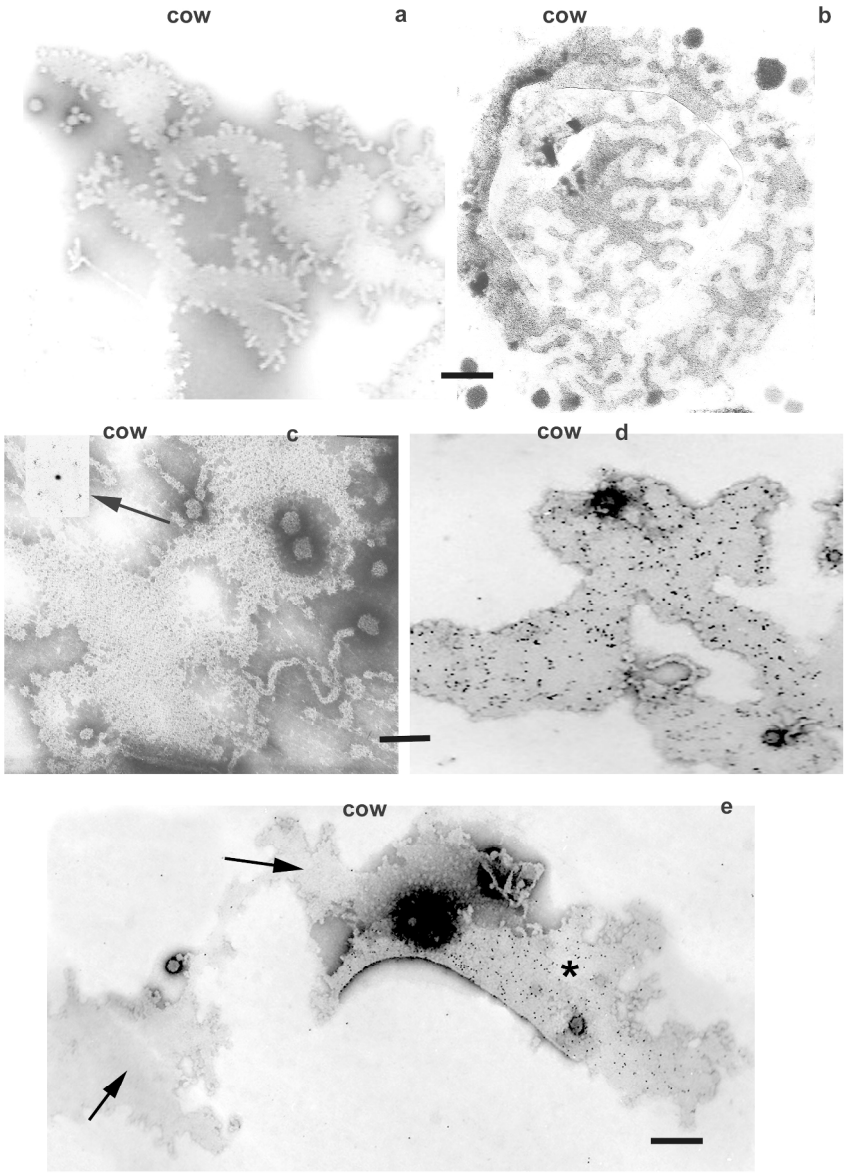

Fig. 8
209x297mm (300 x 300 DPI)

Ultrastructural and immunocytochemical evidence for the reorganisation of the Milk Fat Globule Membrane after secretion.

F. B. Peter Wooding • Ian H Mather

Abstract

This paper reports a detailed ultrastructural and immunocytochemical investigation of the structure of the milk fat globule membrane (MFGM) in a variety of species. The process follows the same pattern in all mammals investigated so far. The initial [or primary] MFGM immediately on release from the mammary cell is a continuous unit membrane with a thin underlying layer of cytoplasmic origin and a monolayer of phospholipid separating it from the core lipid. This structure changes rapidly as the milk fat globule (MFG) moves into the alveolar lumen. The unit membrane plus the underlying layer of cytoplasm modifies drastically into discontinuous patches and networks. These are superimposed upon a continuous apparently structureless sheet of electron dense material stabilising the MFG and similar to that which bounded the lipid in the cell. The underlying layer of the patches increases in electron density, and immunocytochemistry demonstrates localisation of MFGM proteins in this layer. In four species the dense material shows ordered paracrystalline molecular arrays in section and en face views. All the arrays show the same basic pattern and unit size as determined by optical diffraction. Similar patches, networks and arrays are present on the surface of expressed MFG.

Negative staining of lipid extracted expressed MFGs shows similar patches and networks of membrane. These also occasionally show the crystalline arrays and label with MFGM protein antibodies. Similar networks and strands of plasma membrane on the MFG surface are shown by our CLSM examination of unfixed expressed MFG from mice genetically modified to express a fluorescent molecule as a normal plasma membrane constituent.

Keywords: Milk –Fat- Globule- Membrane . Ultrastructure. Immunocytochemistry. Paracrystalline arrays. Unit membrane.

F.B.P. Wooding

Physiology Neuroscience and Development Department, Cambridge University, Cambridge, CB2 3EG, UK

e-mail: fbpw2@cam.ac.uk

I.H. Mather

Department of Animal and Avian Sciences, University of Maryland, College Park, MD20742, USA

List of abbreviations used in the paper:

ADPH Adipohilin(Plin2)

BTN Butyrophilin

CLSM Confocal laser scanning microscopy

EM Electron microscope/ic

FRAP Fluorescence recovery after photobleaching

GFP Green fluorescent protein

MFG Milk fat globule

MFGM Milk fat globule membrane

PMFGM Primary Milk fat globule membrane

RPMFGM Residual Primary Milk fat globule membrane

SMFGM Secondary Milk fat globule membrane

TEM Transmission electron microscopy

XOR Xanthine oxidase

Introduction

According to a recent comprehensive review (Lopez 2011, page 398) the structure of the milk fat globule membrane (MFGM) is "still not known in detail and remains the least understood aspect of the milk fat globule (MFG)".

The functional importance of the MFGM lies in its ability to stabilise the lipid droplets in the milk, facilitate the uptake of MFG components by the neonatal gut, and to supply the developmental cues provided by the biochemical constituents of the membrane. There is increasing evidence (Dewettinck et al 2008; Lopez 2011) for the important role of MFGM constituents in development of the neonatal gut and immune system and in providing antiviral and antimicrobial protection. Longer term the high glycerolipid content could make an important contribution to nervous system development.

The MFGM is also important commercially for its valuable contribution to texture and flavour (Dewettinck et al 2008) given the widespread use of milk and milk derivatives in the food industry.

There are currently two very different interpretations of MFGM structure in the alveolus and in expressed milk. There is general agreement that immediately after secretion from the mammary cell into the alveolus TEM shows that the MFGM is a continuous unit membrane separated from the core lipid by a 15-20 nm layer of cytoplasmic origin. (Wooding 1971; JCS Mather and Keenan 1998; Vorbach et al 2012)

Recent confocal laser scanning microscopy(CLSM) studies of unfixed isolated MFGs from bovine and human milk using lipid probes suggest that the continuous unit membrane persists in the alveolus and after release from the glands. (Evert et al 2008; Gallier et al 2010, 2015; Lopez 2011; Zhang et al 2013)

In contrast most early (Wooding 1971 JUR; Berendsen and Blanchette- Mackie 1979) and more recent TEM results (Armand et al 1996;Gallier et al 2015; can be interpreted to show that there is a drastic rearrangement of the MFGM into discontinuous patches and strands.

This study was designed to distinguish between these two possibilities using a wide range of species and a variety of EM and CLSM techniques.

This paper provides new information on the TEM structure of the MFGM and direct evidence for the reorganisation of the MFGM molecular structure after secretion.

Materials and methods

Electron Microscopy

Mammary tissue from lactating goats, ewes, rats, mice, guinea pigs, fur seals, horses, Friesian or Jersey cows and wallabies was either excised immediately after death by barbiturate overdose and cut into small cubes in an aldehyde, dichromate-acrolein or osmium fixative or fixed initially by perfusion with aldehyde via the mammary artery (cow, ewe, goat, guinea pig and horse). All the processing was carried out at room temperature. Expressed milk was added to an equal volume of fixative.

All animal work was carried out in accordance with the UK Animals (Scientific Procedures) Act 1986 and the Animal Care and Use Committee of the National Institutes of Health, U.S.A. The usual fixation was in 4% glutaraldehyde in 0.1M phosphate buffer, pH 7.2, containing 2% sucrose, for 45 min. Alternatively 1% osmium tetroxide in 0.1M veronal buffer, pH 7-2 or 1.5% acrolein+ 1%potassium dichromate+6%sucrose in 0.1M veronal buffer at 4^{o}C were used.

The tissue was washed briefly in buffer, postfixed first in 1 % osmium tetroxide in 0.1M veronal buffer, pH 7-2, for 30 min, then in 5 % aqueous uranyl acetate for 2 h followed by ethanol dehydration and embedding in Araldite. Sections were cut on an

LKB Ultrotome, stained with uranyl acetate and lead hydroxide and observed in a AEI EM6B electron microscope operated at 60 kV.

.

Electron Microscope Immunocytochemistry.

Tissue was fixed by immersion or perfusion in 4% formaldehyde in 0.1M phosphate buffer, pH 7-2, or in 4% formaldehyde plus 1% glutaraldehyde in 0.1M phosphate buffer, pH 7-2. No osmium was used.

Dehydration and embedding was at room temperature for Araldite resin. Thin sections were cut from the Araldite blocks

and picked up on 300 mesh nickel grids. Resin was removed from the araldite sections by floating for 15 seconds on a solution of one volume of sodium ethoxide (15 grams of sodium hydroxide pellets dissolved in 15 mls of absolute alcohol) diluted with four volumes of distilled water, followed by alcohol and water washes.

For immunocytochemistry the grids were floated overnight section side down on drops of antibody, washed, incubated with immunogold colloid (Goat anti rabbit G10 or 15nm, Jackson Immunoresearch Labs, USA) washed with buffer and water, stained with uranyl acetate and lead solutions and examined in a Philips Electron microscope.

Two primary antibodies were used: rabbit anti BTN (bovine whole molecule, 1:1000) (Banghart et al 1998) and rabbit anti XOR (Bovine whole molecule, 1:100) (Sullivan et al 1982).

Immunocytochemical controls, in which the primary antibody was omitted and replaced with buffer or a non specific antibody at the same concentration, were carried out routinely, alongside the experimental samples. Controls showed an insignificant level of labelling.

Electron Microscope Negative Staining

Freshly expressed uncooled milk was fixed with an equal volume of 4%Glutaraldehyde fixative for 60 min.The fixed milk was spun at ~1500 rpm for 1 min. An EM grid was touched to the surface of a drop of the cream on parafilm, the grid held horizontal for 1 min,then washed with water and dried. The grid was immersed in Heptane for 5 min to remove triglyceride, dried, and negatively stained with a drop of 2% potassium phosphotungstate, the excess blotted off and the grid dried before examination in the EM.

For immunocytochemistry the heptane extracted grid was rehydrated and incubated overnight on XOR antibody, and the

antigen localised with 15 nm gold colloid before negative staining.

Optical diffraction

The micrographs were analysed using a benchtop Optical Diffractometer (Amos 2005) by courtesy of Drs Amos and Richardson, MRC Laboratory of Molecular Biology, Cambridge.

CLSM of mouse MFGs

Milk was collected as described (Ogg et al 2004) from three green fluorescent protein (GFP)-membrane transgenic *mT/mG* mice (Muzumdar et al. 2007) on the tenth day of lactation. Samples of whole milk were immediately incubated at room temperature with BODIPY 650/665 dye (ThermoFisher Scientific) at a final concentration of 10μM for 30 min. This dye stains the triglyceride core of the MFG. Drops of the stained milk were placed on Superfrost/Plus microscope slides, sealed under coverslips and examined with a 60 X oil immersion objective in an Olympus FluoView 1000 confocal microscope. The GFP and BODIPY 650/665 fluorophores were excited at 488 and 633 nm, and emissions collected at 520 and 688 nm, respectively. Optical sections (0.5 μm) through a *z* depth of 10-12 μm were recorded as TIFF files and three dimensional images reconstructed from the *z*-stacks with Imaris

software (Bitplane AG)

Results

Under optimal perfusion conditions (Wooding 1977) in ewe, cow, horse and guinea pig only a few MFGs close or still tenuously attached to the secretory cells show a continuous unit membrane bounding an electron lucent space around the core lipid (Fig 1a ewe; 1b cow; 1c,e horse; 1d,f guinea pig). Further into the alveolar lumen MFGs show a variety of membrane structures most of which can be interpreted as resulting from a disruption and modification of the initial continuous membrane. Mammary tissue optimally fixed by immersion also shows these changes. These changes are coincident with or as a result of alterations in the interactions of the proteins in the material between the membrane and core lipid as indicated by an increase in EM density (Fig 2a, b goat; 2c mouse; 2d pig; 2e,f ewe; 2g cow).

This process produces patches and networks on the surfaces of MFGs with a unit membrane overlying very electron dense material seen on transverse sections on Figure 2. These patches sit upon a continuous dense line, equivalent in EM appearance to the electron dense line which was the lipid core boundary in the cytoplasm. This dense line forms the only continuous structure which stabilised the cytoplasmic lipid droplet in the cell and which now has a similar function in stabilising the secreted MFGs. The area covered by the modified membrane is very variable and different in different species. On sections such

as those on Figure 2, the membrane covers 30-50% of the total area of the MFG in the alveolus in all the species we have examined so far.

The dense line is comparatively thin and difficult to distinguish on low power micrographs (Figs 2a,c; 3a,c arrowheads) but the uniformity of the circularity of the cross sections of the MFG clearly indicate that it is present. At higher magnifications it can be easily seen (Figs 2b,d,g; 3d arrowheads)

The EM evidence for loss of membrane by vesiculation or "blebbing" (Wooding 1971b and Figs 2 e,f) is found in all species examined. A more likely explanation for the drastic morphological change is a contraction of the membrane area presumably driven by an increase in protein molecular order in the dense material under the unit membrane.

For ease of discussion the continuous unit membrane and its adherent layer will be referred to as the Primary MFGM (PMFGM), the dense line as the Secondary MFGM (SMFGM) onto which patches and networks of Residual PMFGM (RPMFGM) are anchored by molecular interactions.

Expressed MFGs show a very similar discontinuous MFGM on TEM examination to those in the alveolus (Fig 3a human; 3b,d cow; 3c wallaby; 3d inset, fur seal): a continuous dense line of SMFGM on which are superimposed RPMFGM patches of unit membrane plus underlying electron dense material. No significant differences have been seen in the structure or percentage of RPMFGM as a result of expression from the gland, and the stability of the membrane in expressed milk has been confirmed by biochemical studies. (Baumrucker and Keeenan 1973)

CLSM micrographs of transverse sections of unfixed expressed MFGs from transgenic mice which constitutively express green fluorescent protein (GFP) on their plasma membrane (Fig 4a, b, c) clearly show an equivalent discontinuous distribution of the RPMFGM-like fluorescence on the contours of the MFGs on transverse sections (compare Figs 2 and 3 with 4a-c). CLSM 3D reconstruction of MFGs demonstrate very similar patches and networks of membrane on their surfaces (Fig 4d -f) equivalent to those on the electron micrographs on Figures 5 and 6.

The close similarity in MFGM structure between all species examined is emphasized by the occurrence of a paracrystalline organisation in the dense material under the unit membrane in some alveolar luminal and expressed MFGs of four unrelated

species. On Fig 5 this can be seen in both en face (5a,c,e cow alveolar; 5b horse milk; 5c goat milk; 5d human milk) and transverse sections (5f, g cow alveolar) of the MFG. The en face EM views on Figures 5 and 6 clearly show the patch and network distribution of the RPMFGM which characteristically show a variety of edge structures including “finger fringed” edges (Figs 5a,c; 6c; 8a,b). The evidence of a change to a greater molecular order in the dense material supports the idea of a post secretion contraction of the original PMFGM producing the patches and networks.

The paracrystalline lattice is based on a similar hexagonal organisation and unit size with similar spacing in all species where it is found, as determined by optical diffraction techniques (Fig 5a-g, 8c). It is not dependant on a primary glutaraldehyde fixation, the same pattern is also produced in the cow MFGM by initial fixation in dichromate–acrolein (Fig 5e) or in osmium (results not shown).

TEM serial section reconstruction of cow alveolar MFGs on Fig 6 show that small circular areas free of RPMFGM can often be clearly recognised.

Immunocytochemical labelling of the sections with antibodies to MFGM proteins shows that only the dense material of the RPMFGM labels, the continuous dense line enveloping the whole MFG is unlabeled (Fig 7a,b). Emphasizing the difference between the two areas of SMFGM, when Ruthenium Red is used to probe for any glycocalyx on the outer surface of the MFG, again the label is only on the RPMFGM unit membrane area of the SMFGM (Fig 7c).

The reality of this membrane structure is reinforced by TEM examination of negatively stained membrane from individual, fixed isolated expressed MFGs (Figs 8a,c,d,e) . Extraction of the core lipid from MFGs adherent to a carbon coated EM grid and subsequent negative staining with Phosphotungstic Acid or Uranyl Acetate reveal membrane patches with finger fringing

(Fig 8a) equivalent to those demonstrated en face (Fig 8b) on EM sections.

Prior incubation of the lipid extracted membrane patches with antibodies to MFGM proteins localised with gold colloid either show dense or no label (Figs 8d,e), presumably depending on which side of the membrane patch was uppermost, this assumption is supported by the observation that where membrane is partially folded back on itself during preparation, only one side of the fold is labelled (Fig 8e).

Occasionally the negatively stained membrane patches show a similar paracrystalline organisation to that demonstrated on the sections (Fig 8c) and OD analysis (inset, arrow) shows a similar hexagonal pattern and unit size to the section material.

Discussion

This paper establishes for the first time in a variety of mammalian genera using a range of TEM and light microscope techniques the uniformity of the detailed structural changes characteristic of the MFGM after secretion from the mammary cell. This confirms and considerably extends the primary author's original studies (Wooding 1971a, b; 1977a,b). The unit membrane which packages the cytoplasmic lipid droplet is necessary to permit continuous release of lipid without damaging the mammary cell. The ingenious solution of collaboration between Golgi vesicles and plasmalemma (Wooding and Sargeant 2015) provides the considerable amount of packaging membrane (Mather 2011) required for MFGM formation.

Once the MFG is released from the cell then the continuous unit membrane is apparently unnecessary and interactions between the MFGM proteins are sufficiently strong to cause the

considerable modification and contraction of the area of the unit membrane with its underlying protein layer. This produces the isolated finger fringed patches and networks of RPFGM on the SMFGM. This process occurs rapidly and describes 90% of the alveolar MFGs. Stability of the MFG is then dependant solely on the SMFGM which forms a continuous envelope equivalent to that which originally bounded the lipid in the cytoplasm. It appears as a continuous dense line on EM sections and is stable enough to survive expression from the mammary gland and storage.

This process of alveolar PMFGM reorganisation occurs in all species so far examined with optimally fixed EM samples and the uniformity of the modifications are exemplified by the equivalence of the paracrystalline structures in the dense material underneath the unit membrane in cow, goat, horse and human. The first report and illustration of paracrystalline areas in finger fringed PMFGM patches was described in cow sectioned material (Wooding 1977a, Figs34, 35; Wooding 1977b).The reality of such membrane structure has subsequently been confirmed by Bucheims freeze fracture studies (Bucheim 1982; 1986; Schmidt and Buchheim 1992) showing very similar images of equivalent unit size. The freeze fracture images were produced from unfixed milk with no glycerol added by ultra rapid cryofixation (Buchheim 1982) yet the micrographs show equivalent RPMFGM patches including some with paracrystalline arrays. These are very similar to those shown in this paper by conventional TEM processing. We consider Buchheim's results with freeze fracture more reliable than Robenek et al 2006 whose localisations and images do not agree with results in the literature.

There are three papers with TEM micrographs which corrobate the discontinuities in MFG in expressed milk.(Berendson and Blanchette –Mackie 1979, rat; Armand et al 1996 and Gallier et al 2015, both human). There are also two papers using TEM claim that alveolar (Freudenstein et al 1979,bovine) and freshly expressed milk

Vorbach et al 2002, mouse)have all or most of the MFG covered with PMFGM. Unfortunately neither paper has micrographs showing several MFG at sufficient resolution to distinguish RPMFGM from SMFGM plus higher magnification of detail with unit membrane resolved such as in figures 2 and 3 in this paper. This is necessary to allow independent judgement of claims of membrane continuity.

In this paper immunocytochemical results from sections confirms that MFGM proteins including BTN and XOR are present in the dense material, and this is reinforced by the MFGM antibody-gold colloid labelling of the negatively stained RPMFGM areas.

Most of the results above are EM section based, and all require prior sample fixation with chemicals. We believe the structure and changes in the MFGM illustrated above are an accurate representation of the normal process in alveolar and expressed milk MFGs. Our conclusions are based on (1) perfusion of tissue providing simultaneous rapid optimal fixation throughout, **producing spherical lipid droplets with unit membranes well resolved,** (2) the fact that all species examined show the same transition **on the same section from** PMFGM to SMFGM plus RPMFGM with the production of very similar paracrystalline organisation in the residual frequently finger fringed RPMFGM areas in four of them, and (3) the equivalent structures demonstrable in negatively stained and freeze fractured specimens. It is also important to note that the PMFGM transition plus crystalline arrays can be found after using three very different primary fixatives: Glutaraldehyde, Osmium or Dichromate –Acrolein.

The most likely proteins to interact to form the unit structure of the paracrystalline arrangements are BTN, XOR and ADPH. (Ishii et al (1995), (Jeong et al 2009), and MacManaman et al (2002) In addition, FRAP analysis showed that a fraction of endogenously expressed GFP-BTN was immobile in condensed areas on the surface of mouse MFGs,

suggesting incorporation into a macromolecular complex (Jeong et al 2013). The immunocytochemical results in this and our previous (Wooding and Sargeant 2015) paper clearly demonstrate the presence of BTN and XOR only in the PMFGM with ADPH throughout the SMFGM.

The nature of the apparently structureless areas of the SMFGM lacking an intact unit membrane is less certain. At a minimum, these regions will comprise the phospholipid monolayer covering the entire globule surface and present on all cellular lipid droplets (Martin and Parton 2006), the PAT family protein ADPH (Chong et al 2011, Jeong et al 2013, Wooding and Sargeant 2015). There may be other proteins (Walther and Farese 2012), including elements of the outer phospholipid bilayer of the PMFGM that were not incorporated into the paracrystalline regions

. Corroboration of the reality of the PMFGM to SMFGM plus RPMFGM transition is provided by the results from unfixed mouse MFGs from the endogenously GFP expressing *mT/mG* strain. The GFP- fluorophore can be considered a marker for intact bilayer membrane (Muzumdar et al 2007). There is a striking equivalence between the confocal images of GFP in transverse sections and 3D reconstructions marking regions of intact bilayer and the morphology of the RPMFGM areas identified on the electron micrographs. Furthermore, when a GFP-BTN fusion protein was expressed in mouse mammary gland using an adenoviral vector, a fraction of the endogenously produced protein condensed on the surfaces of secreted droplets in similar patterns (Jeong et al 2013)

These CLSM results are very similar to those (Evers et al 2008; Gallier et al 2010, 2015; Lopez et al 2010, Lopez 2011; Zhang et al 2013) using exogenous fluorescent lipid or lectin probes to label the unfixed MFG surfaces from bovine or human milk. The results with both markers show

discontinuities (nonfluorescent microdomains) which divide the fluorescence into "patches and networks"(Lopez et al 2010).Lopez interprets these frequently circular nonfluorescent microdomains as local aggregates of molecules (e.g.sphingomyelin) which exclude the probes but with no immunocytochemical evidence for this as yet. Evers considers the domains to indicate the lack of a unit membrane which would agree with our TEM observations. Our serial reconstructions of MFGs show similar circular areas (Fig 6) corresponding to the domains without unit membrane bound RPMFGM .

The uniformity of the detail of this PMFGM formation and transition to SMFGM plus RPMFGM in all species examined at sufficient resolution reinforces the idea that the unique lipid secretion mechanism and subsequent modification method evolved only once in the mammalian lineage. The argument that it is not possible to generalise about the mechanism of MFG secretion because only a small number of mammals have been examined (Heid and Keenan 2005) seems to be contradicted by the similarities in the detail now available in all metatherian and eutherian species adequately investigated.

Acknowledgments

Dr. Roberto Weigert (NCI, NIH) is thanked for supply of the *mT/mG* transgenic mice and permission to use the Olympus confocal microscope.

References

Amos B (2005) Novel

Benchtop Optical Diffractometer for analysis of high resolution TEM images. Microscopy and Analysis 19: 5-7.

Armand M, Hamosh M, Mehta MR, Angelus PA, Philpott JR, Henderson TR, Dwyer NK, Lairon D, Hamosh P (1996) Effect of human milk or formula on gastric function and fat digestion in the preterm infant. Ped Res 40: 429-456.

Banghart LR, Chamberlain CW, Velarde J, Korobko IV, Ogg SL, Jack LJW, Vakharia VN, Mather IH (1998) Butyrophilin is expressed in mammary epithelial cells from a single-sized messenger RNA as a type 1 membrane glycoprotein. J. Biol. Chem. 273: 4171-4179.

Baumrucker CR, Keenan TW (1973) Membranes of the Mammary gland VII. Stability of the MFGM in secreted milk. Biochem Biophys Acta 56: 1092-1099.

Berendson P R, Blanchette-Mackie E J (1979) Milk lipid absorption and chylomicra formation in the suckling rat. Anat Rec 195: 397-414.

Buchheim W (1982) Paracrystalline arrays of MFGM associated proteins as revealed by freeze fracture. Naturwissenschaften 69:505-506.

Buchheim W (1986). Membranes of milk fat globules – ultra-structural, biochemical and technological aspects. Kieler Milchwirtschaftliche Forschungsberichte 38:227-246.

Chong BM, Reigan P, Mayle-Combs KD, Orlicky DJ, McManaman JL (2011) Determinants of adipophilin function in milk lipid formation and secretion. Trends in Endocrinology and Metabolism 22:211-217.

DeWettinck K, Rombaut R, Thienpont N, Trung Le T, Messens K, Van Camp J (2008) Nutritional and technological aspects of MFGM material. Int Dairy Journal 18: 436-457.

Evers JM, Havercamp RG, Holroyd,SE, Jameson GB, Mackenzie DDS, McCarthy OJ (2008) Heterogeneity of MFGM structure and composition as observed using fluorescence techniques. Int Dairy Journal 18: 1081-1089.

Gallier S, Gragson D, Jimenez-Flores R, Everett D (2010) Using CLSM to probe the MFGM and associated proteins. J Agric Food Chem 58: 4250-4257.

Gallier S, Vocking K, Andries Post J, Van De Heijning B, Acton D, Van Der Beek em, Van Baalen T (2015) A novel infant formula concept: Mimickingthe human milk fat globule structure. Colloids and Surfaces B: Biointerfaces 136: 329-339.

Heid HW, Keenan TW (2005) Intracellular origin and secretion of MFG. Eur J Cell Biol 84: 245-258.

Jeong J, Rao AU, Xu J, Ogg SL, Hathout Y, Fenselau C, Mather

IH (2009) The PRY/SPRY/B30.2 domain of butyrophilin 1A1 (BTN 1A1) binds to xanthine oxidoreductase. Implications for the function of BTN 1A1 in the mammary gland and other tissues. J. Biol. Chem. 284:22444-22456.

Jeong J, Lisinski I, Kadegowda AKG, Shin H, Wooding FBP, Daniels BR, Schaack J, Mather IH (2013). A test of the current models for the mechanism of milk-lipid droplet secretion. Traffic 14:974-986.

Lopez C, Madec M, Jimenez-Flores R (2010) Lipid rafts in the MFGM revealed by the lateral segregation of phospholipids and heterogeneous distribution of glycoproteins. Food Chem 120: 22-33.

Lopez C (2011) MFG enveloped by their biological membrane. Unique colloidal assemblies with a specific composition and structure. Curr Opinion in Colloid & Interface Science 16: 391-404.

Mather IH (2000). A review and proposed nomenclature for major proteins of the Milk Fat Globule Membrane. J. Dairy Science 83:203-247.

Mather IH (2011). 'Secretion of milk constituents' in Fuquay JW et al. (eds.) Encyclopedia of Dairy Science, Vol 3, Academic Press: Waltham, pp. 373-380.

Mather IH, Keenan TW (1998) Origin and secretion of milk lipids. J Mammary Gland Biol Neoplasia: 3, 259-273.

Muzumdar MD, Tasic B, Miyamichi K, Li L, Luo L, (2007) A global double-fluorescent Cre reporter mouse, Genesis 45:593-605.

Ogg SL, Weldon AK, Dobbie L, Smith AJH , Mather IH (2004)

Expression of butyrophilin (Btn1a1) in lactating mammary gland is essential for the regulated secretion of milk-lipid droplets. Proc. Natl. Acad. Sci. (U.S.A.) 101:10084-10089.

Robenek H, Hofnagel O, Buers I, Lorkowski S, Schnoor M, Robenek MJ, Heid H, Troyer D, Severs NJ, (2006) Butyrophilin controls milk fat globule secretion. Proc. Natl. Acad. Sci. (U.S.A.) 103:10385- 10390.

Schmidt DG, Buchheim W (1992) The application of Electron Microscopy in dairy research. Journal of Microscopy 167: 105-121.

Sullivan CH, Mather IH, Greenwalt DE, Madara PJ (1982) Purification of xanthine oxidase from the fat-globule membrane of bovine milk by electrofocusing. Determination of isoelectric points and preparation of specific antibodies to the enzyme. Mol. Cell Biochem. 44:13-22.

Vorbach C, Scriven A, Capecchi M (2002) The housekeeping

gene Xanthine Oxidoreductase is necessary for milk fat droplet enveloping and secretion: gene sharing in the lactating mammary gland. Genes and Development 16: 3223-3235.

Walstra P, Jenness R (1984) The MFGM. In: Dairy Chemistry and Physiology, Chapter 5.3 Wiley New York.

Walther TC, Farese RV (2012) Lipid droplets and cellular lipid metabolism. Annu. Rev. Biochem. 81:687-714.

Wooding FBP (1971a). The mechanism of secretion of the Milk Fat Globule. J Ultrastructure Res 9:805-821.

Wooding FBP (1971b). The structure of the MFGM. J Ultrastructure Research 37:388-400.

Wooding FBP (1977a). Comparative mammary fine structure, in Peaker M (ed.) Comparative aspects of lactation. Academic Press: New York, pp. 1-41

Wooding FBP (1977b).Ultrastructural studies on the formation

and fate of the MFGM. Bioc Soc Transactions 5: 61

Wooding FBP, Sargeant TJ (2015) Immunocytochemical evidence for Golgi vesicle involvement on MFG secretion. J Histo Cyto 63: 943-951.

Yang Y, Zheng N, Zhao X, Han R, Ma L, Zhao S, Li S, Guo T, Wang J (2015) Proteomic characterisation and comparison of MFGM proteomes by iTRAC analysis. J Proteomics 116:34-43.

Zheng H, Jimenez-Flores R, Everett D (2013) Bovine MFGM proteins are affected by centrifugal washing processes. J Agric Food Chem 61: 8403-8411.

Figure Legends

Fig. 1 TEM of MFGs from a variety of genera just before (fig 1a) and immediately after (fig 1b – f) release from the mammary cell. Each is bounded by a continuous unit membrane with an inner thin weakly stained cytoplasmic layer enveloping the lipid droplet. All MFGs on figs 1e and 1f showed this PMFGM structure at sufficient magnification as illustrated in the inset on fig. 1f. Bars: a,c,d 50nm; b 75nm; e,f 1µm

Fig. 2 TEM of alveolar MFGs from a variety of genera. All the MFGs show a discontinuous RPMFGM consisting of a unit membrane overlying a cytoplasmic layer of considerably increased electron density (arrows). These RPMFGM patches and networks are supported by a continuous dense line (arrowheads) around each MFG. Examples of a loss of PMFGM by vesiculation (figs 2 e,f) can be found in a small but significant number of MFG in all genera. Bars: a,b,c,d,g 1µm; e,f, 50nm

Fig. 3 TEM of transverse sections of MFGs from expressed milk from a variety of genera demonstrating very similar RPMFGM discontinuities and increases in electron density of the cytoplasmic layer as in the alveolar MFGs. Figure 3d shows two examples at higher magnification illustrating the unit membrane of the discontinuous RPMFGM (arrows) covering the electron dense layer and the single dense line of the SMFGM (arrowheads) enveloping the lipid core. Bars: a,b,c 1μm; d 50nm

Fig. 4 CLSM of MFGs in expressed milk from the GFP-membrane (*mT/mG*) mouse; (a-c) Two dimensional CLSM images showing (a) GFP fluorescence (b) BIODIPY 665 fluorescence of neutral lipid in the MFG (c) Overlay of a and b. Note that the GFP-membrane fluorescence is associated with most of the MFG but in many cases is unevenly distributed on the surface: asterisks show MFG with very little GFP fluorescence on this plane of section, arrows MFG with~ 50% and arrowheads ~100%. (d-f) CLSM of MFGs in three-dimensional reconstructions showing uneven but global distribution of GFP-membrane fluorescence on MFG surfaces.

Compare the GFP distribution on the MFG at the arrows with the TEM images of the MFG surface on Figure 6. (e) BIODIPY 665 fluorescence of neutral lipid in the MFGs, (f) overlay of d and e. Bars, (a-c)20 μm, (d-f) 20 μm.

Fig. 5 TEM of paracrystalline arrays in the RPMFGM. (a – e) En face views of the MFGM from a variety of genera all illustrating the paracrystalline arrays. (f, g)Transverse section views establish the exact location of the arrays in the dense layer underlying the unit membrane. The similarity of the organisation of each en face micrograph is emphasised by their optical diffraction patterns (inset on each) showing hexagonal patterning with equivalent unit sizes. Figs 5a – d and 5f and 5g were all initially fixed in glutaraldehyde, but the same organisation is found after initial dichromate – acrolein fixation of the cow mammary gland (fig 5e). Similar results were obtained with osmium (results not shown). Bars: all 20nm.

Fig. 6 Reconstructions of RPMFGM structure from TEM serial sections of MFGs. The drastic modification of the originally continuous membrane produces a variety of structures, but all show one or more small circular areas free of RPMFGM, similar in size to the areas found by CLSM. Fig.5c also shows large areas (arrows) of paracrystalline organisation in the RPMFGM. Bars: a,b 50nm; c 100nm.

Fig. 7. (a) TEM immunolocalisation of BTN on the cow RPMFGM (between arrows) but not on the dense line (between arrowheads) which is part of the SMFGM. Fig 7b shows the discontinuous distribution of the BTN label on human MFGs, very similar to the discontinuous pattern of RPMFGM on fig. 3a. The section staining is insufficient to clearly distinguish RPMFGM and SMFGM, but at higher magnification in the inset the interruption in the gold colloid labelling is clear between the arrows.

Fig.7c is from cow milk fixed with 500ppm of Ruthenium red added to the aldehyde fixative. The glycocalyx is clearly shown (arrows) on the outside of the RPMFGM unit membrane, no label is apparent on the SMFGM (arrowheads). Bars: a, inset on b, c 50nm; b 1µm

Fig. 8. TEM of cow MFGM negatively stained with phosphotungstic acid. (a) Negatively stained lipid extracted MFG demonstrating the membrane sheets of characteristic outline very similar to RPMFGM as seen en face on sectioned material on (b). (c) The negatively stained RPMFGM sheet shows a similar paracrystalline organisation to that found on the sectioned MFG. Inset at arrow; optical diffraction pattern. (d) TEM immunocytochemistry using 10nm gold particles to demonstrate the distribution of XOR in the MFGM. Some, but not all, of the negatively stained RPMFGM sheets on a grid can be immunolabeled with XOR (or BTN, results not shown) antibodies suggesting that only one side of the sheet labels. Where such membrane sheets are folded back the 10 nm immunolabel is only seen on one side (compare the areas

indicated by the arrow and asterisk on (e)) confirming this hypothesis. Bars: All 50nm.